Fractional-Order PID Controller Design for Time-Delay Systems Based on Modified Bode's Ideal Transfer Function

NIE ZHUO-YUN[ID]1, ZHENG YI-MIN[ID]1, WANG QING-GUO[ID]2, (Member, IEEE), LIU RUI-JUAN3, AND XIANG LEI-JUN[ID]1

[1]School of Information Science and Engineering, National Huaqiao University, Xiamen 361021, China
[2]Institute of intelligent system, University of Johannesburg, Johannesburg 2146, South Africa
[3]School of Applied Mathematics, Xiamen University of Technology, Xiamen 361024, China

Corresponding author: Zheng Yi-Min (zh_even@sina.com)

ABSTRACT This paper proposes a design method for a robust fractional-order PID (FOPID) controller for time-delay systems. A new Bode's ideal transfer function is introduced to tolerance the time-delay in loop. Robust stability is analyzed for the Bode's model in terms of gain and phase margins to help the parameter tuning. To simplify FOPID design from solving nonlinear equations, five unknown parameters are reduced to one in the Bode shaping by data fitting between a parametric model and the real plant. Then, the problem is simply solved by one-dimensional searching. Furthermore, the proposed FOPID controller design is extended to multi-input and multi-output (MIMO) systems by using disturbance observer (DOB). Finally, simulation results are presented to show the effectiveness of the proposed method.

INDEX TERMS Fractional order PID controller, time-delay system, Bode's ideal transfer function, bode shaping.

I. INTRODUCTION

In the past decades, an increasing number of studies are focusing on the application of fractional calculus in many areas of industrial engineering. Fractional system provides a better understanding of system characteristics for many phenomena such as heat transfer [1] and wave propagation [2]. Due to the reliable system description, fractional-order (FO) model have been paid more and more attention in the academics. A recent survey on fractional system is presented in [3], [4] and its applications are introduced in [5], [6]. In the control community, Oustaloup [7] introduced the FO algorithm for the control system and demonstrated superior performance.

In the industry and engineering, proportional-integral-derivative (PID) controller still serves as the most widely used controller because of its simple structure and easily tuning [8], [9]. To improve robustness and performance,

The associate editor coordinating the review of this manuscript and approving it for publication was Nasim Ullah[ID].

Podlubny [10] proposed a generalized PID controller, called FOPID, including a fractional integrator and differentiator. This new form, FOPID, has success among research because of its flexibility and robustness. Some literature has shown the better response of this controller, in comparison with the classical integer PID controller [11], [12]. Different from the classical linear integer–order PID (IOPID) controller, FOPID controller is nonlinear naturally regarding the fractional order, which brings the main difficulties in system design and analysis.

Nowadays, various design methods have been proposed for FOPID controller tuning [13]–[19]. The well–known Ziegler-Nichols tuning rule has been extended to FOPID controller with S-shaped step response, but it only works well on some lag–dominant process [18]. For a typical first-order-plus-dead-time model, some tuning rules are developed to minimize integrated absolute error (IAE) subject to a constraint on the maximum sensitivity [19]. To obtain good control performance, dominant pole placement for FOPID controller is developed based on D-decomposition method [15]. In the

last years, the internal-model-control (IMC) tuning method is also introduced in the design of FOPID controller [16], [17].

Bode shaping is an effective method for control system design in frequency domain [20]–[26] As a good open-loop model, Bode's ideal transfer function is discussed in [22], which shows its stronger robustness against loop gain variation. To realize auto-tuning of PID controller, online optimization technologies are employed to optimize the Bode's model [20] and controller parameters [21]. Due to the robustness to the gain variation, Bode shaping in the frequency domain is also used in the FOPID controller design [22]–[24] by imposing the open-loop phase to be flat in a frequency band. In [24], a model-based analytical method is developed for FOPID controller design via internal model control (IMC) principle and Bode's model. In [25], a robust FOPID controller tuning strategy is developed based on the flat phase property and optimal Bode's model. This popular scheme can also be found in [13], [14], which is based on the robustness specifications, including the desired phase margin, gain crossover frequency and the flatness of the phase Bode plot. However, for time-delay process, Bode shaping become complicated since the selection of Bode model is constrained by the time-delay item, and often results in complex analytical design and numerical optimization [26], which motivate us to investigate the Bodel's transfer function design and its parameter selection for time delay system in FOPID design.

Time-delay is often encountered in industrial engineering, such as the chemical process and networked control system [27], and often brings in great difficulty in control system design. For example, networked control systems are typical time-delay systems and the time-delay introduced by the network inevitably makes the system performance degraded and may even damage the system stability [28], [29]. Although many modern control strategies have been developed for time-delay systems, PID control is considered as a simple yet effective manner to possess great robustness against system time-delay [30]–[32]. In recent years, an increasing number of studies can be found related to FOPID control for time-delay systems. The basic idea to cope with time-delay is to design a robust controller that can tolerate the time-delay in the feedback control loop. In [33], an analytical approach for the design of FOPID controller is proposed on the basis of the IMC scheme and the maximum sensitivity for FO systems with time-delay. As time-delay systems have infinite-dimensional property naturally, the design of the FOPID controller is more complex than the delay-free case. Thus, finding the set of stabilizing FOPID controller parameters for time-delay systems has been paid great attention. Several methods [12], [34], [35] have been proposed to draw the stability boundary graphically in parameter space based on the D-decomposition method with stability margin specifications [36].

In this paper, we aim to propose a robust FOPID controller design for time-delay systems by Bode shaping. To realize this goal, two problems are solved in this paper:

A new Bode's ideal transfer function is design to tolerance the time-delay in loop. We select a time delay Bode's model for FOPID design. It is well known that, the bandwidth design for time-delay system is a critical problem in control system design. However, this problem is seldom discussed in the current Bode shaping methods [37], [38]. We solve this problem by investigating the gain and phase margins for the proposed time-delay Bode's model.

Bode shaping for FOPID design is solved by one-dimensional searching, rather than five parameter optimizations. To simplify the design of FOPID from solving nonlinear equations, data fitting at steady state and the crossover frequency are derived, such that five unknown parameters are reduced to one. Then, the problem is easily solved by one–dimensional searching.

The rest of this paper is organized as follows. Section 2 shows the preliminaries. Section 3 describes the proposed FOPID design method. Section 4 extends the proposed method to multivariable systems. Section 5 illustrates comparative numerical results. Finial, Section 6 concludes this study with final remarks.

II. PRELIMINARIES
A. FRACTIONAL CALCULUS
Fractional calculus is a generalization of the integration and differentiation to the non-integer order operator. The differ-integral operator, denoted by $_aD_t^\alpha$, is defined by

$$_aD_t^\alpha = \begin{cases} \dfrac{d^\alpha}{dt} & \alpha > 0 \\ 1 & \alpha = 0 \\ \displaystyle\int_a^t (d\tau)^{-\alpha} & \alpha < 0, \end{cases} \tag{1}$$

where $\alpha \in R$ is the order of the operator and a and t are called lower and upper terminal, respectively. There are several definitions for fractional derivatives [23], [39], such as Grünwald-Letnikov (G-L) and Riemann-Liouville (R-L) definitions. As one of the most commonly used definitions, G–L fractional differential/integral definition has the form [39]:

$$_aD_t^\alpha f(t) = \lim_{h \to 0} h^{-\alpha} \sum_{j=0}^n \omega_j^{(\alpha)} f(t - jh), \tag{2}$$

where h is the step size, $n = (t - a)/h$, representing the number of sampling points in a time interval $[a, t]$, and $\omega_j^{(\alpha)} = (-1)^j \begin{pmatrix} \alpha \\ j \end{pmatrix}$ is a polynomial coefficient of the sampling signal $f(t - jh)$, with $\begin{pmatrix} \alpha \\ j \end{pmatrix} = \frac{\alpha!}{j!(\alpha-j)!}$. Note, that, fractional operator is a nonlocal operation over an interval $[a, t]$, i.e. the operator symbol $_aD_t^\alpha$ is explicitly expressed over the upper and lower terminals.

While the R-L definition is written as

$$
\begin{aligned}
&_aD_t^\alpha f(t) \\
&= \begin{cases} \dfrac{1}{\Gamma(n-\alpha)}\dfrac{d^n}{dt^n}\displaystyle\int_a^t \dfrac{f(\tau)}{(t-\tau)^{\alpha-n+1}}d\tau, & n-1<\alpha<n \\[2mm] \dfrac{1}{\Gamma(-\alpha)}\displaystyle\int_a^t \dfrac{f(\tau)}{(t-\tau)^{\alpha+1}}d\tau, & \alpha<0, \end{cases}
\end{aligned}
\tag{3}
$$

where $\Gamma(\cdot)$ is Euler's gamma function. The Laplace transform of the R-L fractional derivative/integral (3) under zero initial conditions for the order $\alpha(0 < \alpha < 1)$ is presented as

$$
\mathcal{L}\left\{_aD_t^{\pm\alpha}f(t)\right\} = s^{\pm\alpha}F(s)
\tag{4}
$$

One point should be emphasized is that, for a wide class of functions, the G-L and R-L definitions are equivalent [39].

B. FOPID CONTROLLER

The generalized transfer function of the FOPID controller is first introduced by Podlubny [10], and is defined as follows

$$
G_c(s) = k_p + \frac{k_i}{s^\lambda} + k_d s^\mu,
\tag{5}
$$

where k_p is the proportional gain, k_i is the integration gain, and k_d is the derivative gain; λ and μ are the integral and derivative orders, respectively, satisfying $0 < \lambda, \mu < 2$. It can be easily found that, by selecting $\lambda = \mu = 1$, a standard IOPID controller is obtained. As discussed in [39], the FOPID owns an important feature that it allows for a continuous slope compensation of the controller's Bode plot both at low and high frequencies, depending, respectively, on λ and μ. Thus, this feature can be utilized for a more effective loop shaping and better control performance [22], [23]. However, the problem is also raised by these two additional order parameters, which results in complex controller tuning rules in practice because the FOPID transfer function is nonlinear with respect to the coefficients λ and μ.

C. BODE'S IDEAL TRANSFER FUNCTION

An ideal open-loop transfer function is proposed in [22], that is

$$
L(s) = \left(\frac{\omega_c}{s}\right)^\alpha, \quad \alpha \in \mathbb{R},
\tag{6}
$$

where ω_c is the gain crossover frequency of $L(s)$, and $0 < \alpha < 2$ is a real. The parameter α determines both the slope of the magnitude curve on Bode plot and the phase margin of the system. In the Bode diagrams, the amplitude of $L(s)$ is a straight line of constant slope $-20\alpha\, dB/dec$, and its phase curve is a horizontal line at $-\alpha\pi/2\, rad$, which indicates the Bode's ideal transfer function $L(s)$ possesses strong robustness against gain variation. It means that the variation of the process gain only changes the crossover frequency ω_c but maintains the phase margin constant $\pi(1 - \alpha/2)rad$.

The robustness against gain variation is commonly used in FOPID design as an additional specification [13], [14], [24], [35], which demands that the phase Bode plot of the designed
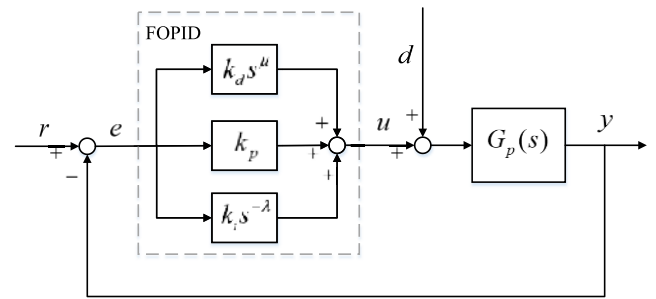

FIGURE 1. FOPID control system.

open-loop system $G(s)$ is flat around the gain crossover frequency ω_c

$$
\left|\frac{dArg\,(G\,(j\omega))}{d\omega}\right|_{\omega=\omega_c} = 0,
$$

Therefore, this specification requires the exact phase formulation of the open-loop system being explicit to the frequency variable.

The choice of $L(s)$ as open-loop transfer function also gives an ideal closed-loop model under a unit feedback

$$
F(s) = \frac{\omega_c^\alpha}{s^\alpha + \omega_c^\alpha},
\tag{7}
$$

with infinite gain margin and constant phase margin.

III. THE PROPOSED METHOD
A. BASIC IDEA

The block diagram of the FOPID control system is shown in Fig.1, where $G_p(s)$ is the controlled plant. The following time-delay system is considered in this paper,

$$
G_p(s) = G_0(s)e^{-Ts},
\tag{8}
$$

where T is the time-delay, and $G_0(s)$ is the normal model delay–free. With FOPID, the closed-loop system is given by

$$
\frac{G_p(s)G_c(s)}{1 + G_p(s)G_c(s)} = \frac{G_0(s)G_c(s)}{1 + G_0(s)e^{-Ts}G_c(s)}e^{-Ts}.
\tag{9}
$$

Note that the time-delay item always appears in the closed-loop system (9). Combined with the Bode's ideal transfer function and the time-delay item, a desired closed-loop model for time-delay systems is chosen as

$$
H(s) = \frac{\omega_c^\alpha}{s^\alpha + \omega_c^\alpha}e^{-Ts},
\tag{10}
$$

such that the time-delay in $H(s)$ equals to the real one.

Aimed at the desired closed-loop model $H(s)$, suppose there is an process model $\tilde{G}_p(s)$, satisfying

$$
H(s) = \frac{\tilde{G}_p(s)G_c(s)}{1 + \tilde{G}_p(s)G_c(s)},
\tag{11}
$$

We have

$$
\tilde{G}_p(s) = \frac{H(s)}{G_c(s) - H(s)G_c(s)}
$$

$$
= \frac{\omega_c^\alpha s^{\lambda-\alpha} e^{-Ts}}{\left(k_p s^\lambda + k_i + k_d s^{\mu+\lambda}\right)\left[1 + \frac{\omega_c^\alpha (1 - e^{-Ts})}{s^\alpha}\right]}
$$

$$
= \frac{\omega_c^\alpha s^{\lambda-\alpha}}{\left(k_p s^\alpha + k_i + k_d s^{\mu+\alpha}\right)} [1 - \Delta(s)] e^{-Ts}, \quad (12)
$$

where

$$
\begin{cases} 1 - \Delta(s) = 1 - \dfrac{\varphi(s)}{1 + \varphi(s)} = \dfrac{1}{1 + \varphi(s)} \\ \varphi(s) = \dfrac{\omega_c^\alpha}{s^\alpha}(1 - e^{-Ts}). \end{cases}
$$

Note that, $\tilde{G}_p(s)$ in (12) can be viewed as a parametric model of $G_p(s)$, since all the five unknown parameters of FOPID and as well as two parameters of the desired model are appearing explicitly in (12). The basical idea for the FOPID controller design is to solve all the unknown parameters to make the parametric model $\tilde{G}_p(s)$ closed to the real plant $G_p(s)$ by data fitting. Some optimal searching algorithms, such as particle swarm optimization [40] and neural network [41], can be used to solve the problem. The main difficulties will come from three aspects:

1) The parametric model $\tilde{G}_p(s)$ in (12) is an infinite–dimensional system because of the time-delay involved in $\Delta(s)$;
2) The nonlinear optimization with multi-parameter often falls into the local optimality.
3) No stabilization controller can be found if the desired model inappropriate.

To develop a simple yet effective design method, some prior knowledge of the process is assumed and employed in the design. Two assumptions are made on the process: 1) the plant $G_p(s)$ is stable, and 2) the plant has a nonzero steady value, $G_p(j0) \neq 0$. These two assumptions are satisfied in most of industry processes.

B. APPROXIMATE ROBUST STABILITY ANALYSIS

It is well known that the specified control performance can be achieved by feedback control for delay–free systems theoretically. Different from this case, the stability and control performance of time-delay systems is physically limited by the time-delay in the closed-loop. Intuitively, bandwidth, say ω_c, cannot be arbitrary large under the limitation of time-delay or sampling time.

Denote the frequency response of a transfer function $W(s)$ as $W(j\omega)$. With assumptions discussed previously, data fitting at the steady–state requires $\tilde{G}_p(j0) = G_p(j0) \neq 0$, yielding $\lambda - \alpha = 0$ and

$$
\tilde{G}_p(s) = \frac{\omega_c^\alpha}{\left(k_p s^\alpha + k_i + k_d s^{\mu+\alpha}\right)} [1 - \Delta(s)] e^{-Ts}. \quad (13)
$$

Observing the parametric model $\tilde{G}_p(s)$ in (13), it is obvious that limiting $|\Delta(s)|$ in a small value can reduce the difference between $\tilde{G}_p(s)$ and $G_p(s)$ to benefit the data fitting. In this manner, given a small constant ε, satisfying $0 < \varepsilon < 1$, and specified $\|\Delta(s)\|_\infty < \varepsilon$, the possible choice of ω_c should

satisfy

$$
\omega_c^\alpha \leq \left(\frac{\varepsilon}{1-\varepsilon}\right) / \left\|(1 - e^{-Ts})/s^\alpha\right\|_\infty. \quad (14)
$$

Assuming that data fitting will be carried on with the constraint in (14), to have $G_p(s) \approx \tilde{G}_p(s)$. In this way, the open-loop transfer function satisfies

$$
G_p(s)G_c(s) \approx \tilde{G}_p(s)G_c(s) = \frac{\omega_c^\alpha e^{-Ts}}{s^\alpha}(1 - \Delta(s)). \quad (15)
$$

Recalling that $\|\Delta(s)\|_\infty < \varepsilon$ and ε is a small positive constant, we have

$$
G_p(s)G_c(s) \approx \frac{\omega_c^\alpha e^{-Ts}}{s^\alpha}(1 - \Delta(s)) \approx \frac{\omega_c^\alpha e^{-Ts}}{s^\alpha}. \quad (16)
$$

As discussed previously, a system with the Bode's ideal transfer function owns a finite gain margin and constant phase margin. However, this merit is changed by the time-delay item of the process. Based on the approximation in (16), the gain and phase margins of $G_p(s)G_c(s)$ are expressed by

$$
A_m \approx \left\| \left(\frac{(2-\alpha)\pi}{2T\omega_c}\right)^\alpha \right\|, \quad (17)
$$

$$
\gamma = (\pi - \frac{\alpha}{2}\pi - T\omega_c)rad = (180 - 90\alpha - 57.3T\omega_c)^o, \quad (18)
$$

respectively. To guarantee the closed-loop stability, it requires $A_m > 1$ and $\gamma > 0$, to have

$$
\omega_c < \frac{\pi}{T} - \frac{\alpha\pi}{2T}, \quad (19)
$$

when $0 < \alpha < 2$.

The approximate stability analysis presented above is meaningful because it provides some guidelines to select two important parameters in (10). Furthermore, (17) and (18) give the estimation on the stability margins. We can design them (A_m and γ) large enough to guaranteed the closed-loop stability. Several remarks are given to show the details.

Remark 1: The developed conditions in (14) and (19) can be viewed as stability constraints in the proposed FOPID design. The selection of α and ω_c based on (14) and (19) guarantees the existing of stabilized FOPID as well as the closed-loop performance.

Remark 2: The closed-loop bandwidth has a major impact on the system overshoot, response speed, and disturbance rejection performance. (14) and (19) provides an analytical result on the performance limitation by the time-delay of a control system. A suitable closed-loop bandwidth selection benefits a successful controller with closed-loop stability and performance guaranteed.

Remark 3: the analytical results on the stability in (17) and (18) reveal a fact that a large closed-loop bandwidth will reduce the gain and phase margins of time-delay systems. One can also specify the robustness stability based on (17) and (18) to have $A_m > A_m^*$ and $\gamma > \gamma^*$, where A_m^* and γ^* are the specified gain and phase margins, respectively.

C. CONTROLLER DESIGN

This paper presents a simple yet effective FOPID design in the frequency domain with one-dimensional searching. Based on the discussion in [22], $\alpha \approx 1$ is recommended for the trade-off between fast response and small overshoot. Therefore, the remaining bandwidth parameter ω_c is selected under the stability constraints in (14) and (19).

Note that, the real plant $G_p(s)$ may have high-order dynamic or uncertainties. The parametric model $\tilde{G}_p(s)$ can be viewed as its reduced-order nominal model which dominants the dynamic characteristic of $G_p(s)$. We make data fitting in a certain frequency range $[0, \omega_x]$, where ω_x is selected at the phase crossover frequency of $G_p(s)$, such that $\angle G_p(j\omega_x) = -\pi$. Procedures of the proposed FOPID design are given as following.

Step 1: Set $\alpha \approx 1$ and select ω_c under the stability constraints (14) and (19) for good robustness in terms of the gain and phase margins in (17) and (18), respectively;

Step 2: Data fitting at the steady state. Let $\tilde{G}_p(j0) = G_p(j0) \neq 0$. With the integral order $\lambda = \alpha$, the integration gain k_i is derived

$$k_i = \frac{\omega_c^\alpha}{\left(1 + \omega_c^\alpha \lim_{s \to 0} \frac{1-e^{-Ts}}{s^\alpha}\right) G_p(j0)}. \quad (20)$$

Step 3: Data fitting at the phase crossover frequency $\omega = \omega_x$. Let $\tilde{G}_p(j\omega_x) = G_p(j\omega_x)$, that is

$$\frac{\omega_c^\alpha}{\left(k_p j^\alpha \omega_x^\alpha + k_i + k_d j^t \omega_x^t\right)} = \frac{G_p(j\omega_x)}{(1 + \Delta(j\omega_x)) e^{-Tj\omega_x}} = p + qj, \quad (21)$$

where

$$\begin{cases} t = \alpha + \mu \\ p = Re\left[\dfrac{G_p(j\omega_x)}{(1 + \Delta(j\omega_x)) e^{-Tj\omega_x}}\right] \\ q = Im\left[\dfrac{G_p(j\omega_x)}{(1 + \Delta(j\omega_x)) e^{-Tj\omega_x}}\right], \end{cases}$$

Using Euler's formula, j^α and j^t are expressed as

$$j^t = a + jb, \quad j^\alpha = c + jd,$$

where $a = \cos\left(\frac{\pi}{2}t\right)$, $b = \sin\left(\frac{\pi}{2}t\right)$, $c = \cos\left(\frac{\pi}{2}\alpha\right)$ and $d = \sin\left(\frac{\pi}{2}\alpha\right)$. Then, equation (16) yields

$$\begin{cases} k_d(\mu) = -\dfrac{(dp + cq)\omega_x^\alpha k_p + k_i q}{(pb + qa)\omega_x^t} \\ k_p(\mu) = \dfrac{bk_i(p^2 + q^2) - (pb + qa)\omega_c^\alpha}{(da - cb)(p^2 + q^2)\omega_x^\alpha}. \end{cases} \quad (22)$$

Till now, two parameters λ and k_i are determined. k_d and k_p are well formulated with the variable μ. Further calculation for the derivative order μ is by one–dimensional searching to realize model matching.

Step 4: Data fitting in the frequency range $(0, \omega_x)$. The fitting error in the frequency range $(0, \omega_x)$ can be numerically

expressed by

$$J = \sum_{\omega=0}^{\omega_x} \left| G_p(j\omega) - \tilde{G}_p(j\omega) \right|^2. \quad (23)$$

We can minimize J to determine the value of μ in the range of $0 < \mu < 2$

$$\min_{0 < \mu < 2} J = \sum_{\omega=0}^{\omega_x} \left| G_p(j\omega) - \tilde{G}_p(j\omega) \right|^2. \quad (24)$$

In (22), k_d and k_p can be uniquely determined if μ is iterated. In this way, the design of FOPID is solved in (24) by one-dimensional searching technology.

IV. EXTENSION TO MIMO SYSTEM

Consider the FOPID design for $n \times n$ MIMO systems $G(s)$. Suppose the diagonal elements of $G(s)$ are $\{G_{p1}(s), G_{p2}(s), \cdots, G_{pn}(s)\}$. The system outputs can be expressed as $Y = [y_1, y_2, \cdots, y_n]^T$ with

$$y_i = G_{pi}(u_{g_i} + d_i + w_i), \quad i = 1, 2, \cdots, n,$$

where u_{g_i} is the input signal for i-th loop, d_i is the external disturbance and w_i is the equivalent coupling disturbance caused by the other loops. Obviously, the coupling disturbance w_i will affect the control performance greatly, which is the major difficulty in MIMO control system design.

Recently, the decoupling control by disturbance observer (DOB) has been well discussed and demonstrated in [44]. The diagonal element G_{pi} is considered as a single loop system in DOB design such that the total disturbance $d_i + w_i$ can be estimated and compensated in real time. A diagonal element G_{pi} is firstly decomposed into a minimum phase transfer function, $g_q(s)$, and a non-reversible function $g_p(s)$, containing input/output time-delay or NMP elements with unity gain. Suppose that $\tilde{g}_q(s)$ is the nominal model of $g_q(s)$. The low-pass filter $Q_i(s)$ with unity gain is used to ensure the physical realization of $Q(s)\tilde{g}_q^{-1}(s)$. The transfer function from u to y can be simply calculated by

$$G_{pi}(s) = \frac{g_q(s)\tilde{g}_q(s)}{[1 - Q_i(s)g_p(s)]\tilde{g}_q(s) + Q_i(s)g_p(s)g_q(s)} g_p(s) \quad (25)$$

Note that, if $\left|1 - Q_i(s)g_p(s)\right|$ is shaped zero in a wide frequency range, $G_{pi}(s)$ can be recovered as its nominal model $g_p(s)\tilde{g}_q(s)$, that is $G_{pi}(s) \approx g_p(s)\tilde{g}_q(s)$. Thus, the proposed FOPID can be applied to $G_{pi}(s)$ directly. Based on the DOB decoupling, the proposed FOPID for MIMO system in each loop is shown in Fig.2. The design procedures will be discussed in the simulation study in details.

V. SIMULATIONS

In this section, some typical plants, including first-order-plus-time-delay (FOPTD) system, second-order-plus-time-delay (SOPTD) system and uncertain system, are used to illustrate the effectiveness of the proposed method.
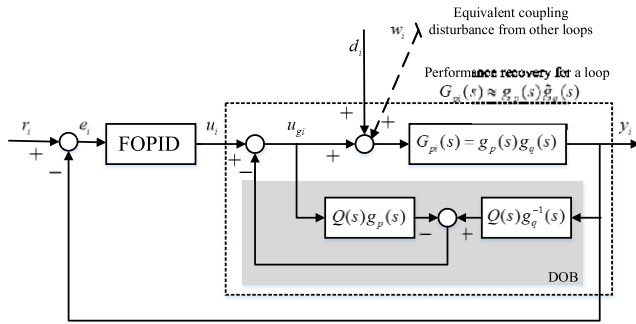
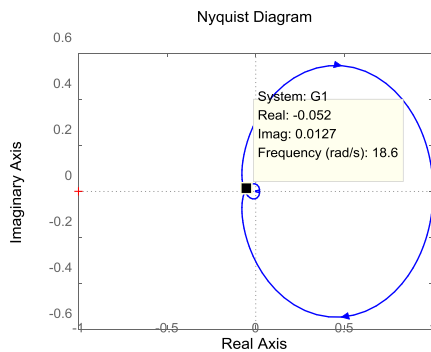**FIGURE 2. FOPID for MIMO system with DOB decoupling.**

FIGURE 3. The Nyquist of $G_1(s)$.

FIGURE 4. Step responses using controllers in (28)–(30).
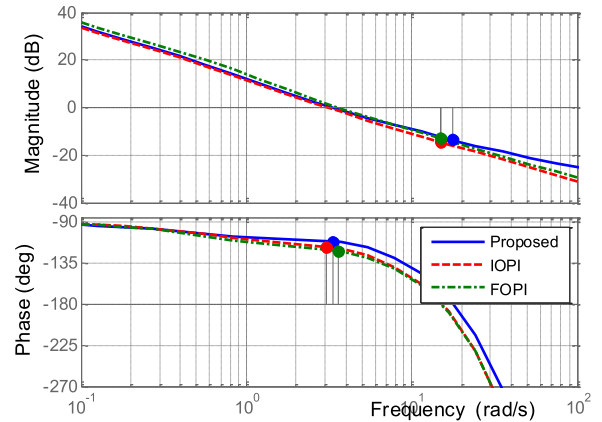
FIGURE 5. Bode diagrams with the controllers (28)–(30).

Comparisons are made to some existing methods. Some metrics are used to evaluate controller performance, including, gain margin A_m, phase margin γ, gain crossover frequency ω_γ, overshoot σ, rise time t_r, settling time t_s and ISE index

$$ISE \int_0^\infty e^2(t)dt. \tag{26}$$

A. EXAMPLE 1; FOPTD SYSTEM

Consider a FOPTD system in literature [35]

$$G_1(s) = \frac{1}{s+1}e^{-0.1s}. \tag{27}$$

We set $\varepsilon = 0.36$. With the stability constraints in (14) and (19), the parameters $\omega_c = 4.85$ and $\alpha = 1.01$ are selected. The gain and phase margins are estimated by (17) and (18) respectively, that is $A_m \approx 3.2$ and $\gamma \approx 61^o$.

Then, the integration gain k_i is derived to have $k_i = 4.9272$. As $\omega_x = 18.6$ determined in Fig.3, the optimization is carried on for (24) and the differential order is determined $\mu = 0.68$. We calculate the remaining parameters by (22), and the finial FOPID controller is obtained

$$C_{T=0.1}(s) = 3.1534 + \frac{4.9272}{s^{1.01}} + 0.1487s^{0.68}. \tag{28}$$

For this process, an integer order (IO) PI controller is optimized following the recognized method by Astrom and Hagglund [42] as
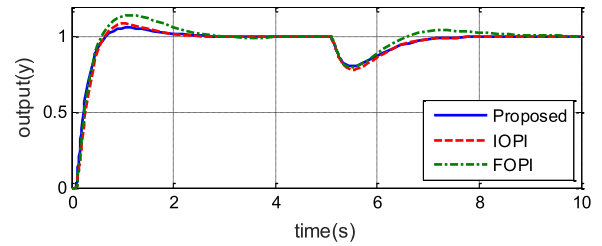
$$C_{IOPI}(s) = 2.8236 + \frac{4.6464}{s}, \tag{29}$$

and an FO proportional–integral (FOPI) controller is designed to fulfill a flat phase constraint by Luo [35] as

$$C_{FOPI}(s) = 3.3367 + \frac{4.6464}{s^{1.21}}. \tag{30}$$

To illustrate the set-point tracking and disturbance rejection performance, step response and load disturbance response are presented in Fig.4. Clearly, the proposed FOPID in (28) provides better control performance than the controllers in (29) and (30), which is also demonstrated by their frequency response of open-loop transfer functions in Fig.5.

All the compared indexes are shown in Table 1 for the set-point response. The effectiveness of the proposed method can also be observed that the achieved gain and phase margins in Table 1 are closed to the estimated ones in (17) and (18).

To compare the robustness of three controllers, the step responses with $\pm 20\%$ loop gain variations are presented in Fig.6. The performance shows the system robustness to the gain uncertainties using the proposed FOPID controller. Compared with the step responses using the controllers (29) and (30), the overshoots of the proposed FOPID are smaller and with shorter settling time.

For further investigation, the proposed FOPID design is tested for different time-delay cases, $T = 0.3$ and $T = 0.5$. Two FOPID controllers are obtained as follows

$$C_{T=0.3}(s) = 0.405 + \frac{3.1104}{s^{0.85}} + 0.7895s^{0.529}, \tag{31}$$
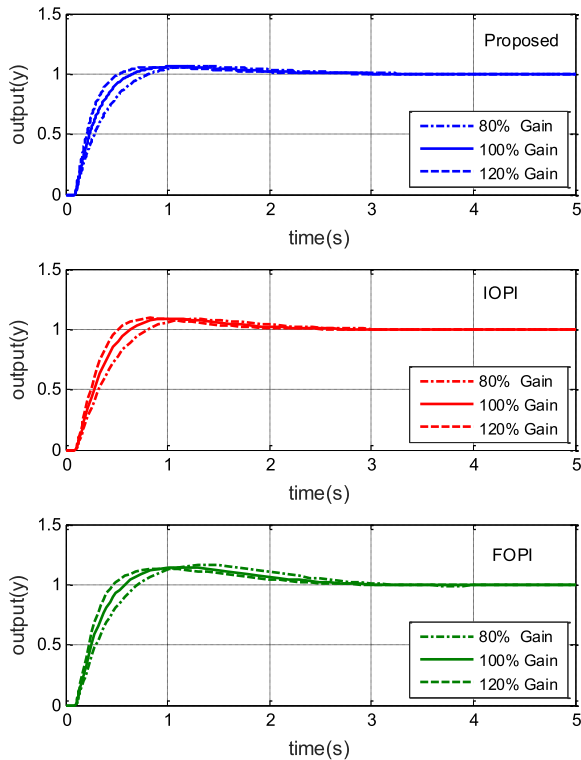
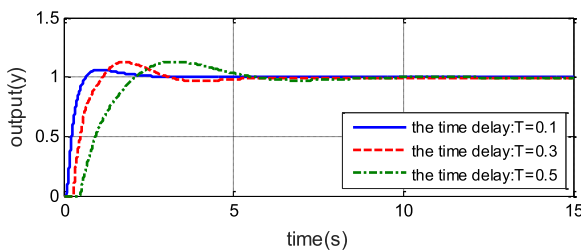**FIGURE 6. Step responses with open-loop gain variations ±20%.**

FIGURE 7. Step responses of the control system using controllers in (28), (31) and (32).

TABLE 1. Frequency and time domain performance for example 1.

Controllers	A_m	γ (deg)	ω (rad/s)	(%)	t_r (s)	t_s (s)	ISE
Proposed	4.78	67.8	3.35	6.05	0.39	2.38	7.897
Astrom	5.3	62.3	3.06	8.74	0.38	2.19	8.098
Ying Luo	4.46	57.5	3.62	14.64	0.38	2.58	8.184

and

$$C_{T=0.5}(s) = 0.5728 + \frac{1.458}{s^{0.93}} + 1.231 s^{0.24}. \quad (32)$$

The step responses are shown in Fig.7 for the control systems with (28), (31) and (32). It is obvious that, with proper parameter selection for ω_c and α, the proposed method is applicable to large time-delay case.
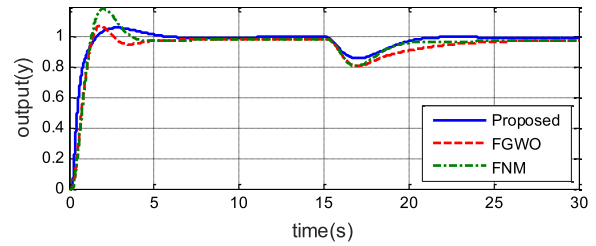
FIGURE 8. Step responses using controllers in (34)–(36).

B. EXAMPLE 2: SOPTD SYSTEM

Consider the SOPTD system in literature [43]

$$G_2(s) = \frac{0.5}{2s^2 + 3s + 1} e^{-0.2s}, \quad (33)$$

$\varepsilon = 0.36$ is set to limit the value of $\Delta(s)$ in (16). We select $\omega_c = 2.5$ and $\alpha = 0.98$ for the robust stability according to (14), (17)–(19). The gain and phase margins are estimated by (17) and (18) respectively, that is $A_m \approx 3.12$ and $\gamma \approx 63.15^o$.

The crossover frequency $\omega_x = 2.77$ is determined by the Nyquist plot of $G_2(s)$. The proposed FOPID controller is calculated by data fitting in the frequency range $[0, \omega_x)$, to have

$$C_{proposed}(s) = 10.0796 + \frac{4.9092}{s^{0.98}} + 7.0213 s^{1.064}. \quad (34)$$

Optimal searching algorithms are often used to solve the design problem of FOPID. In this example, we illustrate the effectiveness of (34) compared with two optimal FOPID controllers in [43], using Grey wolf optimization (FGWO) and Nelder's-Mead optimization (FNM), respectively:

$$C_{FGWO}(s) = 5.8208 + \frac{3.3408}{s^{0.75712}} + 5.5551 s^{0.65412}, \quad (35)$$

$$C_{FNM}(s) = 0.055 + \frac{7.4342}{s^{0.51094}} + 8.2837 s^{0.50076}. \quad (36)$$

Fig. 8 shows the step and load disturbance responses of three resultant control systems. The control performances are compared in Table 2. The results demonstrated that, compared to five parameters searching schemes, one-dimensional searching used in this paper also provides a satisfactory control performance but with a simple calculation. The Bode plots are shown in Fig. 9, which shows a larger phase margin of the proposed FOPID (34) and the flatness of the phase plot.

For further investigation on the robustness of three controllers, Fig.10 shows the step responses when ±40% gain variation occurring in the open-loop plant. The simulation results indicate the proposed FOPID owns better robustness on the gain variation than the controllers (34) and (35). This result can be well understood due to the flatness on the phase plot providing more robustness to gain variation.

C. EXAMPLE 3: UNCERTAIN SYSTEM

In this example, the real system is:
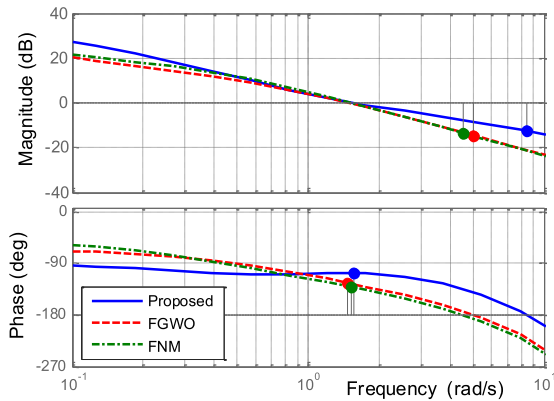
$$G_3(s) = \frac{1}{(s+1)^4}. \quad (37)$$

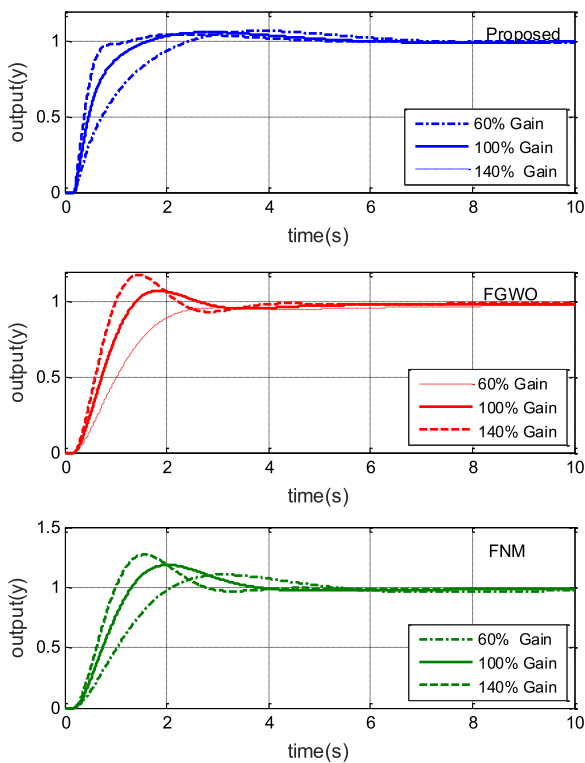**FIGURE 9. Bode diagrams with the controllers (34)–(36).**

FIGURE 10. Step responses with open-loop gain variations ±40%.

TABLE 2. Frequency and time domain performance for example 2.

Controllers	A_m	$\cdot$	ω		t_r	t_s	ISE
		(deg)	(rad/s)	(%)	(s)	(s)	
Proposed	4.26	73.62	1.562	6.14	0.83	5.34	0.147
FGWO	5.43	56.27	1.479	7.44	0.27	5.05	0.206
FNM	4.73	48.13	1.535	18.6	0.26	6.25	0.221

As discussed in [37], this plant can be approximated by the following time-delay low-order model

$$G_4(s) = \frac{0.22287e^{-0.5532s}}{s^{2.2251} + 0.86316s^{1.0389} + 0.22394}. \quad (38)$$
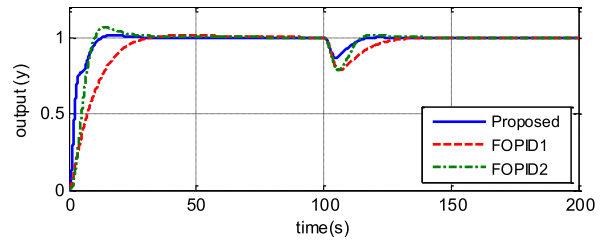

FIGURE 11. Step responses and load disturbance responses of the control system using controllers in (39)–(41).
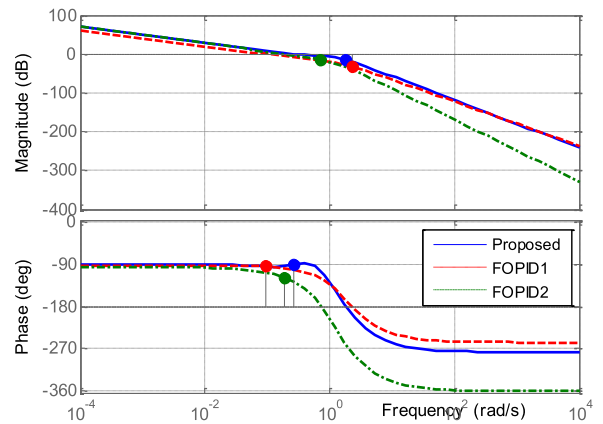

FIGURE 12. Bode diagrams with the controllers (39)–(41).

We use (38) as the nominal model to design the FOPID controller. With the selection of $\varepsilon = 0.36$, $\omega_c = 0.3$ and $\alpha = 1.01$, the proposed FOPID is designed

$$C_{proposed}(s) = 0.9403 + \frac{0.2964}{s^{1.01}} + 1.7067s^{0.923}. \quad (39)$$

For the comparison, the FOPID controllers using the methods in [37] and [38] are obtained as

$$C_{FOPID1}(s) = \frac{0.3252}{s^{0.0369}}\left(1 + \frac{0.2594}{s^{1.0389}} + 1.1585s^{1.1862}\right), \quad (40)$$

$$C_{FOPID2}(s) = 0.3677 + \frac{0.0781}{s^{1.1204}} + \frac{0.0992}{s^{1.0158}}, \quad (41)$$

respectively.

Simulation comparisons are carried on for the real plant (37). Fig.11 shows the step responses and load disturbance responses. The corresponding control performances are given in Table 3. It can easily be seen that both the step response and disturbance rejection performance are better than two compared FOPID controllers. These results are also supported by their frequency response in Bode plots, as shown in Fig. 12. The open-loop system using the FOPID controller (39) provides a larger phase crossover frequency to generate a fast system response and a flatness of phase plot around $\omega = \omega_c$.

As a robustness analysis, the step responses of the three FOPID controllers in Fig. 13 are obtained when the open-loop system has ±50% gain variations. It can be seen that even large gain variation occurring, the control performance still maintains quite well.
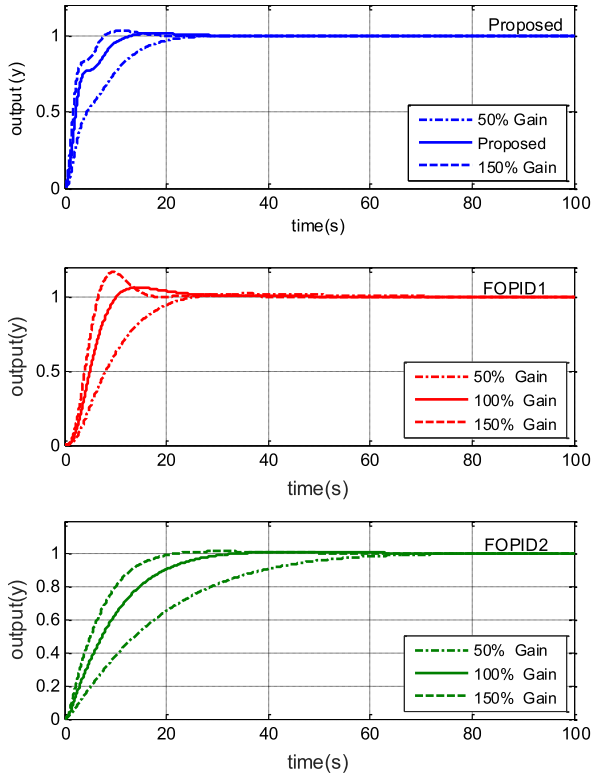
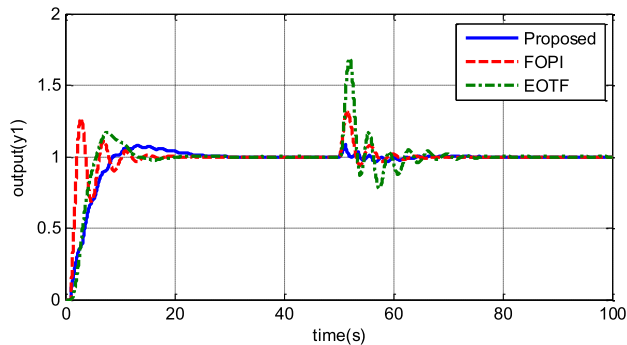**FIGURE 13.** Step responses with open-loop gain variations ±40%.

FIGURE 14. Closed-loop responses to the sequential step changes in the set-point for the VL column (loop1).

D. EXAMPLE 4: MIMO SYSTEM

A 24-tray tower separating a mixture of methanol and water, examined by Luyben [45] has the following transfer function matrix

$$G(s) = \begin{bmatrix} \dfrac{-2.2e^{-s}}{7s+1} & \dfrac{1.3e^{-0.3s}}{7s+1} \\ \dfrac{-2.8e^{-1.8s}}{9.5s+1} & \dfrac{4.3e^{-0.35s}}{9.2s+1} \end{bmatrix} \quad (42)$$

According to section IV, MIMO processes can be compensated by DOB in the inner loops for performance recovery as shown in Fig.2. According to the design method in [44], we select

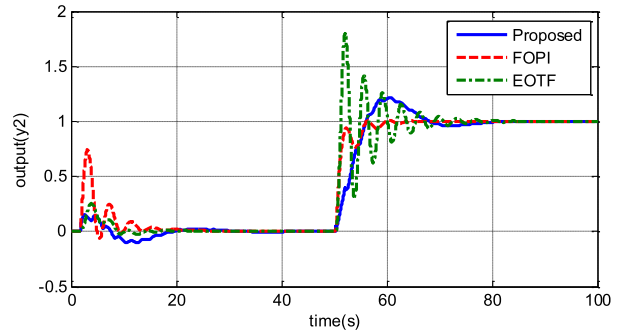$$Q_1(s) = \frac{s+1}{0.1s+1}, \; Q_2(s) = \frac{0.35s+1}{0.5s+1}$$

FIGURE 15. Closed-loop responses to the sequential step changes in the set-point for the VL column (loop2).

TABLE 3. Frequency and time domain performance for example 3.

Controllers	A_m	$\dot{\varphi}$ (deg)	ω (rad/s)	(%)	t_r (s)	t_s (s)	ISE
Proposed	6.1	88	0.272	1.29	7.46	20.56	0.669
Erhan Yumuk	43.1	80.13	0.099	2.04	17.49	49.27	2.244
Das S	5.55	61.36	0.188	6.36	6.11	30.56	1.657

TABLE 4. The optimal fopid values and ISE FOR example 4.

		Kp	Ki	λ	Kd	μ	ISE
Proposed	Loop1	-0.65	-0.141	1.06	-0.212	0.805	0.376
	Loop2	0.455	0.165	0.95	0.091	1.477	0.553
FOPI	Loop1	-2.772	-0.413	1	-	-	0.762
	Loop2	1.955	0.218	1.002	-	-	0.863
EOTF	Loop1	-1.89	0.281	-	-	-	1.048
	Loop2	5.20	0.588	-	-	-	1.273

for loop 1 and loop 2, respectively. Then, we design FOPID controller just like a single loop for the diagonal processes

$$g_1(s) = \frac{-2.2e^{-s}}{7s+1}, \quad g_2(s) = \frac{4.3e^{-0.35s}}{9.2s+1}$$

directly. Consequently, $\varepsilon_1 = 0.36$ and $\varepsilon_2 = 0.5$ are set to limit the value of $\Delta(s)$ in (16). We select $\omega_{c1} = 1.5$, $\omega_{c2} = 0.14$ and $\alpha_1 = 1.06$, $\alpha_2 = 0.95$ for the robust stability according to (14), (17)-(19). The crossover frequency $\omega_{x1} = 5.28$ and $\omega_{x2} = 5.65$ are selected according to the Nyquist plot of $g_1(s)$ and $g_2(s)$. The proposed FOPID controllers are calculated by data fitting between the frequency range $[0, \omega_{x1})$ and $[0, \omega_{x2})$, to have

$$C_{loop1}(s) = -0.652 - \frac{0.141}{s^{1.06}} - 0.212s^{0.805} \quad (43)$$

$$C_{loop2}(s) = 0.455 + \frac{0.165}{s^{0.95}} + 0.091s^{1.477} \quad (44)$$

For this process, we make comparisons to the FOPID design methods in [46] and [47]. The comparison results are depicted in Fig.14, Fig.15 and Table 4. In the simulation study, the step inputs for two loops are set $r_1(t) = 1(t)$ and

$r_2(t) = 1(t - 50)$, respectively. From Figs.14 and 15, we can observe that, the coupling effects between two loops are very strong in the cases of [46] and [47], generate large overshoot and oscillations in two loops response. While in our case, the coupling effects are well overcome by the proposed control scheme, provide good control performance. The results are also confirmed by ISE index in Table 4.

VI. CONCLUSION

This paper presents a simple yet effective FOPID controller tuning method for time-delay systems. A time-delay closed-loop model with Bode's ideal transfer function is introduced for control system design. Robust stability is analyzed in terms of gain and phase margins. Bandwidth selection is a critical problem in time-delay system design but is seldom discussed in the current FOPID works [22], [23], [37], [38]. We give an analytical method to solve this problem based on the proposed stability conditions. To simplify the design of FOPID from solving nonlinear equations, five unknown parameters are reduced to one by data fitting. Then, one-dimensional searching is used to find the solution. Furthermore, the proposed FOPID controller design is extended to MIMO systems. Finally, the effectiveness of the proposed method is illustrated by numerical simulations and comparisons. The further work is to investigate the discretization for fractional operator such that the proposed FOPID controller can be applied in a real control system.
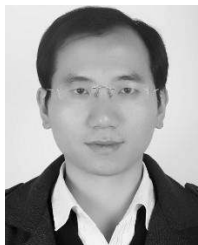
REFERENCES

[1] A. Atangana and D. Baleanu, "New fractional derivatives with nonlocal and non-singular kernel: Theory and application to heat transfer model," *Thermal Sci.*, vol. 20, no. 2, pp. 763–769, 2016.

[2] T. Zhu and J. M. Harris, "Modeling acoustic wave propagation in heterogeneous attenuating media using decoupled fractional laplacians," *Geophysics*, vol. 79, no. 3, pp. T105–T116, May 2014.

[3] Y. Li, Y. Chen, H.-S. Ahn, and G. Tian, "A survey on fractional-order iterative learning control," *J. Optim. Theory Appl.*, vol. 156, no. 1, pp. 127–140, Jan. 2013.

[4] M. Tavazoei, "Time response analysis of fractional-order control systems: A survey on recent results," *Fractional Calculus Appl. Anal.*, vol. 17, no. 2, pp. 440–461, Jan. 2014.

[5] R. Caponetto, G. Maione, and J. Sabatier, "Fractional-order control: A new approach for industrial applications," *Control Eng. Pract.*, vol. 56, pp. 157–158, Nov. 2016.

[6] Z.-X. Zou, K. Zhou, Z. Wang, and M. Cheng, "Frequency-adaptive fractional-order repetitive control of shunt active power filters," *IEEE Trans. Ind. Electron.*, vol. 62, no. 3, pp. 1659–1668, Mar. 2015.

[7] A. Oustaloup, F. Levron, B. Mathieu, and F. M. Nanot, "Frequency-band complex noninteger differentiator: Characterization and synthesis," *IEEE Trans. Circuits Syst. I, Fundam. Theory Appl.*, vol. 47, no. 1, pp. 25–39, Jan. 2000.

[8] Q.-G. Wang, T.-H. Lee, H.-W. Fung, Q. Bi, and Y. Zhang, "PID tuning for improved performance," *IEEE Trans. Control Syst. Technol.*, vol. 7, no. 4, pp. 457–465, Jul. 1999.

[9] L. Sun, J. Shen, Q. Hua, and K. Y. Lee, "Data-driven oxygen excess ratio control for proton exchange membrane fuel cell," *Appl. Energy*, vol. 231, pp. 866–875, Dec. 2018.

[10] I. Podlubny, "Fractional-order systems and $PI^\lambda D^\mu$ controllers," *IEEE Trans. Autom. Control*, vol. 44, no. 1, pp. 208–214, Jan. 1999.

[11] C. A. Monje, B. M. Vinagre, V. Feliu, and Y. Chen, "Tuning and auto-tuning of fractional order controllers for industry applications," *Control Eng. Pract.*, vol. 16, no. 7, pp. 798–812, Jul. 2008.

[12] S. Ethem Hamamci, "An algorithm for stabilization of fractional-order time delay systems using fractional-order PID controllers," *IEEE Trans. Autom. Control*, vol. 52, no. 10, pp. 1964–1969, Oct. 2007.

[13] Y. Luo and Y. Chen, "Fractional order [proportional derivative] controller for a class of fractional order systems," *Automatica*, vol. 45, no. 10, pp. 2446–2450, Oct. 2009.

[14] Y. Luo, Y. Q. Chen, C. Y. Wang, and Y. G. Pi, "Tuning fractional order proportional integral controllers for fractional order systems," *J. Process Control*, vol. 20, no. 7, pp. 823–831, Aug. 2010.

[15] P. D. Mandić, T. B. Šekara, M. P. Lazarević, and M. Bošković, "Dominant pole placement with fractional order PID controllers: D-decomposition approach," *ISA Trans.*, vol. 67, pp. 76–86, Mar. 2016.

[16] B. Maâmar and M. Rachid, "IMC-PID-fractional-order-filter controllers design for integer order systems," *ISA Trans.*, vol. 53, no. 5, pp. 1620–1628, Sep. 2014.

[17] M. Bettayeb and R. Mansouri, "Fractional IMC-PID-filter controllers design for non integer order systems," *J. Process Control*, vol. 24, no. 4, pp. 261–271, Apr. 2014.

[18] D. Valério and J. S. da Costa, "Tuning of fractional PID controllers with Ziegler–Nichols-type rules," *Signal Process.*, vol. 86, no. 10, pp. 2771–2784, Oct. 2006.

[19] F. Padula and A. Visioli, "Tuning rules for optimal PID and fractional-order PID controllers," *J. Process Control*, vol. 21, no. 1, pp. 69–81, Jan. 2011.

[20] B. B. Alagoz, A. Ates, and C. Yeroglu, "Auto-tuning of PID controller according to fractional-order reference model approximation for DC rotor control," *Mechatronics*, vol. 23, no. 7, pp. 789–797, Oct. 2013.

[21] X. Li, Y. Wang, N. Li, M. Han, Y. Tang, and F. Liu, "Optimal fractional order PID controller design for automatic voltage regulator system based on reference model using particle swarm optimization," *Int. J. Mach. Learn. Cybern.*, vol. 8, no. 5, pp. 1595–1605, Oct. 2017.

[22] R. S. Barbosa, J. A. T. Machado, and I. M. Ferreira, "Tuning of PID controllers based on bode?S ideal transfer function," *Nonlinear Dyn.*, vol. 38, nos. 1–4, pp. 305–321, Dec. 2004.

[23] B. Saidi, M. Amairi, S. Najar, and M. Aoun, "Bode shaping-based design methods of a fractional order PID controller for uncertain systems," *Nonlinear Dyn.*, vol. 80, no. 4, pp. 1817–1838, Jun. 2015.

[24] M. Bettayeb, R. Mansouri, U. Al-Saggaf, and I. M. Mehedi, "Smith predictor based fractional-order-filter PID controllers design for long time delay systems," *Asian J. Control*, vol. 19, no. 2, pp. 587–598, Mar. 2017.

[25] L. Liu and S. Zhang, "Robust fractional-order PID controller tuning based on Bode's optimal loop shaping," *Complexity*, vol. 2018, pp. 1–14, Jun. 2018.

[26] T. N. L. Vu and M. Lee, "Analytical design of fractional-order proportional-integral controllers for time-delay processes," *ISA Trans.*, vol. 52, no. 5, pp. 583–591, Sep. 2013.

[27] Y. Wang, P. He, H. Li, X. Sun, W. Wei, Z. Wei, and Y. Li, "Stabilization for networked control system with time-delay and packet loss in both S-C side and C-A side," *IEEE Access*, vol. 8, pp. 2513–2523, 2019, doi: 10.1109/ACCESS.2019.2962076.

[28] Y. F. Wang, Z. X. Li, P. L. Wang and Z. Zhou, "Robust H^∞ fault detection for networked Markov jump systems with random time-delay," *Math. Problems Eng.*, vol. 2017, Aug. 2017, Art. no. 2608140, doi: 10.1155/2017/2608140.

[29] Y.-F. Wang, Z. Li, P. Wang, and Z. Zhou, "Robust H_∞ fault detection for networked control systems with Markov time-delays and data packet loss in both S/C and C/A channels," *Math. Problems Eng.*, vol. 2019, pp. 1–11, Jan. 2019, doi: 10.1155/2019/4672862.

[30] Q.-G. Wang, Z. Ye, W.-J. Cai, and C.-C. Hang, "Multivariable PID control based on dominant pole placement," in *PID Control for Multivariable Processes*. Berlin, Germany: Springer, 2008.

[31] G. Lloyds Raja and A. Ali, "Smith predictor based parallel cascade control strategy for unstable and integrating processes with large time delay," *J. Process Control*, vol. 52, pp. 57–65, Apr. 2017.

[32] D.-J. Wang, "Synthesis of PID controllers for high-order plants with time-delay," *J. Process Control*, vol. 19, no. 10, pp. 1763–1768, Dec. 2009.

[33] D. Li, L. Liu, Q. Jin, and K. Hirasawa, "Maximum sensitivity based fractional IMC-PID controller design for non-integer order system with time delay," *J. Process Control*, vol. 31, pp. 17–29, Jul. 2015.

[34] S. E. Hamamci and M. Koksal, "Calculation of all stabilizing fractional-order PD controllers for integrating time delay systems," *Comput. Math. Appl.*, vol. 59, no. 5, pp. 1621–1629, Mar. 2010.

[35] Y. Luo and Y. Chen, "Stabilizing and robust fractional order PI controller synthesis for first order plus time delay systems," *Automatica*, vol. 48, no. 9, pp. 2159–2167, Sep. 2012.

[36] R. Lanzkron and T. Higgins, "D-decomposition analysis of automatic control systems," *IRE Trans. Autom. Control*, vol. 4, no. 3, pp. 150–171, Dec. 1959.

[37] E. Yumuk, M. Güzelkaya, and I. Eksin, "Analytical fractional PID controller design based on Bode's ideal transfer function plus time delay," *ISA Trans.*, vol. 91, pp. 196–206, Aug. 2019.

[38] S. Das, S. Saha, S. Das, and A. Gupta, "On the selection of tuning methodology of FOPID controllers for the control of higher order processes," *ISA Trans.*, vol. 50, no. 3, pp. 376–388, Jul. 2011.

[39] F. Padula, *Advances in Robust Fractional Control*. Cham, Switzerland: Springer, 2015.

[40] X. Liu, "Optimization design on fractional order PID controller based on adaptive particle swarm optimization algorithm," *Nonlinear Dyn.*, vol. 84, no. 1, pp. 379–386, Apr. 2016.

[41] M. Ö. Efe, "Neural network assisted computationally simple $PI^\lambda D^\mu$ control of a quadrotor UAV," *IEEE Trans. Ind. Informat.*, vol. 7, no. 2, pp. 354–361, May 2011.

[42] K. J. Åström and T. Hägglund, *Advanced PID Control*. Pittsburgh, PA, USA: ISA-The Instrumentation, Systems, and Automation Society, 2006.

[43] S. K. Verma, S. Yadav, and S. K. Nagar, "Optimization of fractional order PID controller using grey wolf optimizer," *J. Control, Autom. Electr. Syst.*, vol. 28, no. 3, pp. 314–322, Jun. 2017.

[44] L. Sun, D. Li, and K. Y. Lee, "Enhanced decentralized PI control for fluidized bed combustor via advanced disturbance observer," *Control Eng. Pract.*, vol. 42, pp. 128–139, Sep. 2015.

[45] W. L. Luyben, "Simple method for tuning SISO controllers in multivariable systems," *Ind. Eng. Chem. Process Design Develop.*, vol. 25, no. 3, pp. 654–660, Jul. 1986.

[46] S. K. Lakshmanaprabu, M. Elhoseny, and K. Shankar, "Optimal tuning of decentralized fractional order PID controllers for TITO process using equivalent transfer function," *Cognit. Syst. Res.*, vol. 58, pp. 292–303, Dec. 2019.

[47] T. N. L. Vu and M. Lee, "Independent design of multi-loop PI/PID controllers for interacting multivariable processes," *J. Process Control*, vol. 20, no. 8, pp. 922–933, Sep. 2010.

ZHENG YI-MIN received the B.S. degree in mechanical and electronic engineering from Fuzhou University, Fujian, China, in 1999, and the Ph.D. degree in control theory and control engineering from Xiamen University, Fujian, in 2018. He joined Huaqiao University, Fujian, in 2005, where he is currently working as a Lecturer with the Department of Control Science and Engineering. His research interests include the field of industrial process control, multivariable systems, decoupling control, fractional-order systems, system identification, and model-based control for complex nonlinear systems.

WANG QING-GUO (Member, IEEE) received the B.Eng. degree in chemical engineering and the M.Eng. and Ph.D. degrees in industrial automation from Zhejiang University, China, in 1982, 1984, and 1987, respectively. He held Alexander-von-Humboldt Research Fellowship of Germany, from 1990 to 1992. From 1992 to 2015, he was with the Department of Electrical and Computer Engineering, National University of Singapore, where he became a Full Professor, in 2004. He is currently a Distinguished Professor with the Institute for Intelligent Systems, University of Johannesburg, South Africa. He has published over 250 international journal articles and six books. He received nearly 11000 citations with H-index of 58. His current research interests are mainly in modeling, estimation, prediction, control, optimization, and automation for complex systems, including but not limited to, industrial and environmental processes, new energy devices, defense systems, medical engineering, and financial markets.
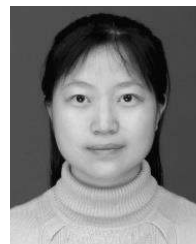
LIU RUI-JUAN received the Ph.D. degree in control theory and control engineering from Central South University, China, in 2014. She was a Visiting Scholar with the University of South Wales. She joined the Xiamen University of Technology, Xiamen, China, in 2014, where she is currently an Associate Professor with the School of Applied Mathematics. Her research interests include robust control, disturbance rejection control, and fractional-order systems.

NIE ZHUO-YUN received the B.Sc. degree in automation and the Ph.D. degree in control theory and control engineering from Central South University, China, in 2006 and 2012, respectively. He was a Visiting Researcher with the National University of Singapore, from 2007 to 2009. He joined Huaqiao University, Xiamen, China, in 2013, where he is currently an Associate Professor of control science and engineering. His research interests are in robust adaptive control, disturbance rejection control, nonlinear systems, and intelligent robot. He was a recipient of *Journal of The Franklin Institute*'s Outstanding Reviewer of 2015.

XIANG LEI-JUN received the M.Sc. degree in mechatronic engineering from the Zhejiang University of Technology, China, in 2005. He joined Huaqiao University, Xiamen, China, in 2005, where he is currently a Lecturer with the College of Information Science and Engineering. His research interests include active disturbance rejection control, fractional-order PID control, and their applications in complex industrial systems.

• • •